Catalytic promiscuity of a proline-based tautomerase

Rahimi, Mehran

CHAPTER 4

MUTATIONS CLOSER TO THE ACTIVE SITE IMPROVE THE PROMISCUOUS ALDOLASE ACTIVITY OF 4-OXALOCROTONATE TAUTOMERASE MORE EFFECTIVELY THAN DISTANT MUTATIONS

Mehran Rahimi, Jan-Ytzen van der Meer, Edzard M. Geertsema, Harshwardhan Poddar, Bert-Jan Baas, and Gerrit J. Poelarends, accepted in *ChemBioChem.* DOI: 10.1002/cbic.201600149

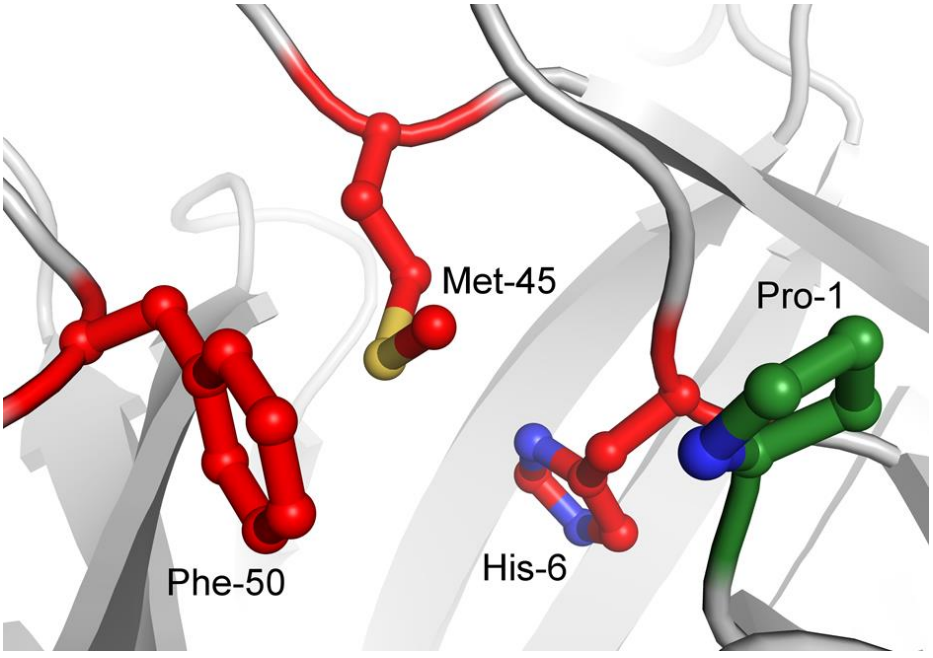

The enzyme 4-oxalocrotonate tautomerase (4-OT), which in nature catalyzes an enol-keto tautomerization step as part of a degradative pathway for aromatic hydrocarbons, promiscuously catalyzes various carbon-carbon bond-forming reactions. This includes the aldol condensation of acetaldehyde with benzaldehyde to yield cinnamaldehyde. Here, we demonstrate that 4-OT can be engineered into a more efficient aldolase for this condensation reaction, with a>5000-fold improvement in catalytic efficiency (in terms of k_{cat}/K_m) and a>10^7-fold change in reaction specificity, by exploring small libraries in which only 'hotspot' positions are varied. These 'hotspot' positions were identified by a systematic mutagenesis strategy, covering each residue position, followed by an initial screen for single mutations that give a strong improvement in the desired aldolase activity. The beneficial mutations were all found to be near the active site of 4-OT, demonstrating that for new catalytic activities in a promiscuous enzyme, mutations closer to the active site improve the enzyme more effectively than distant ones.

4.1 Introduction

The enzyme 4-oxalocrotonate tautomerase (4-OT) is a member of the tautomerase superfamily, a group of homologous proteins that share a β-α-β structural fold and a unique catalytic amino-terminal proline (Pro-1).[1–3] 4-OT catalyzes the conversion of 2-hydroxy-2,4-hexadienedioate (**1**) to 2-oxo-3-hexenedioate (**2**) (Scheme 4.1) as part of a catabolic pathway for aromatic hydrocarbons in *Pseudomonas putida* mt-2.[4,5] In this tautomerization reaction, residue Pro-1 functions as a general base that removes the 2-hydroxyl proton of **1** for delivery to the C-5 position to yield **2**. Pro-1 can function as a general base because the prolyl nitrogen has a pK_a of ∼6.4 and exists largely as the uncharged species at cellular pH.[6]

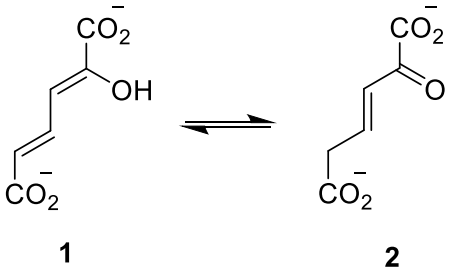

Scheme 4.1: The proton-transfer reaction naturally catalyzed by 4-OT.

In addition to its natural tautomerase activity, 4-OT promiscuously catalyzes several carbon-carbon bond-forming Michael-type addition and aldol condensation reactions.[7–16] This includes the aldol condensation of acetaldehyde (**3**) with benzaldehyde (**4**) to yield cinnamaldehyde (**6**) (Scheme 4.2).[10,12] 4-OT catalyzes both the initial addi-

tion of **3** to **4** to yield 3-hydroxy-3-phenylpropanal (**5**) as well as the subsequent dehydration of **5** to give **6**. 4-OT also catalyzes a retro-aldol reaction with **5** as the substrate, yielding **3** and **4**.[12] $NaCNBH_3$ trapping, mass spectrometry, and X-ray crystallography experiments strongly suggest a mechanism in which Pro-1 functions as a nucleophile, rather than a base, and reacts with the carbonyl functionality of **3** to form a covalent enamine intermediate.[12,17] This intermediate reacts with **4** in an aldol addition. After enzymatic dehydration of **5**, the final product **6** is released from the active site upon hydrolysis. Notably, mechanism-inspired engineering provided an active site mutant (F50A) with enhanced aldol condensation activity (600-fold in terms of k_{cat}/K_m).[12]

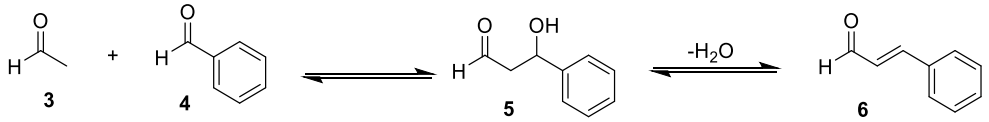

Scheme 4.2: The aldol condensation reaction promiscuously catalyzed by 4-OT.

The adol reaction is one of the most important reactions in synthetic chemistry and has been widely used for the production of valuable compounds.[18–22] Therefore, there is great interest in the development of novel aldolases for biocatalytic applications. In this study, we investigated whether 4-OT can be engineered into a more efficient aldolase by exploring small libraries in which only 'hotspot' positions are varied.

4.2 Results and discussion

Residues that affect activity can be found anywhere in proteins,[23–26] therefore we first applied a systematic mutagenesis strategy to identify residue positions at which mutations give a marked improvement in the aldolase activity of 4-OT. For this, a previously constructed collection of 1040 single mutants of 4-OT,[27] covering at least 15 of the 19 possible variants at each residue position, from Ile-2 to Arg-62, was used. A heat map for the aldolase activity of 4-OT was generated by determining the effect of each mutation on the ability of the enzyme to catalyze the aldol condensation of **3** with **4** to yield **6** (Figure 4.1). Given the low-level aldolase activity of wild-type 4-OT, the activity measurements were performed under screening conditions that allowed only for the detection of variants with strongly improved aldolase activity.

Using this systematic mutagenesis approach, three 'hotspot' positions at which single mutations greatly improve the aldolase activity of 4-OT were identified (Figure 4.1). These include mutations at positions His-6 (Val, Ile, Leu), Met-45 (His) and Phe-50 (Ala, Val, and Ile). Residues His-6, Met-45 and Phe-50 are lining the Pro-1 pocket, illustrating that single mutations close to the active site can strongly improve the promiscuous aldolase activity of 4-OT. The single mutants with the best aldolase activity at each of these residue positions (H6I, M45H, and F50V; see Figure 4.S1) were purified, and their

catalytic performance was compared to that of wild-type 4-OT by transformations using 150 µM enzyme and a 25-fold excess of **3** (50 mM) over **4** (2 mM). Analysis of the progress curves of these reactions showed that the single mutants H6I, M45H and F50V have strongly enhanced aldolase activity for the condensation of **3** with **4** when compared to wild-type 4-OT, with mutant F50V displaying the highest aldolase activity (Figure 4.2 and Figure 4.S2). Notably, no mutations which significantly enhance the aldolase activity of 4-OT were found at distant residue positions.

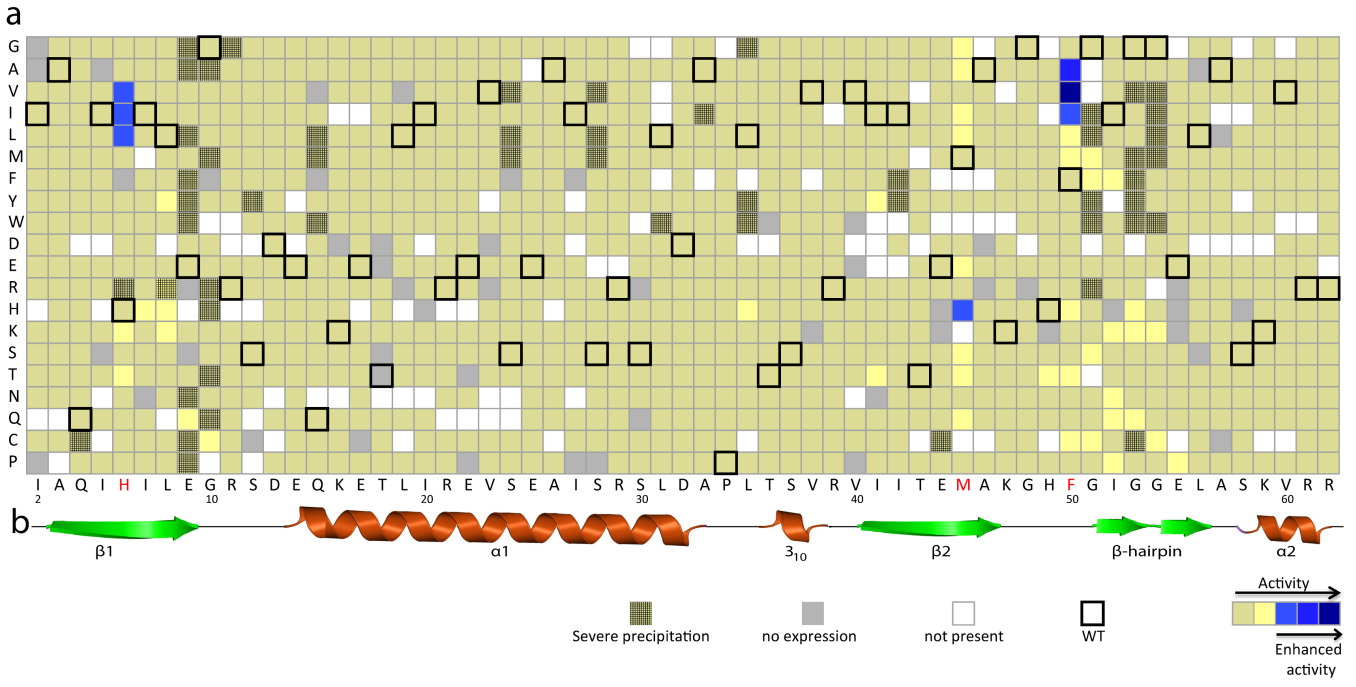

Figure 4.1: Heat map of 4-OT for the aldol condensation of acetaldehyde (**3**) with benzaldehyde (**4**) to yield cinnamaldehyde (**6**). **a)** The horizontal axis of the data matrix depicts the wild-type sequence of 4-OT and the vertical axis depicts the 20 possible amino acid residues. The wild-type amino acid residue at each position is indicated by bold squares, white boxes represent mutants that are not present in the collection, and grey boxes represent mutants that were not produced above the detection limit (<0.5 mg/mL in the cell free extract). Boxes with a crosshatch pattern represent mutants that precipitated under the screening conditions. The ability of the single mutants of 4-OT to catalyze the aldol condensation of **3** with **4** to give **6** was determined by UV-spectroscopy (full details can be found in the Supporting Information). The increases in absorbance at 290 nm, which corresponds to the formation of product **6**, are represented as colors in the data matrix to create a visually interpretable heat map. **b)** The secondary-structure elements of 4-OT.

To investigate whether the three 'hotspot' positions (His-6, Met-45 and Phe-50) are good targets to further enhance 4-OT's promiscuous aldolase activity, these positions were subjected to combinatorial mutagenesis. The NNK-codon degeneracy, covering all 20 possible amino acids, was used for randomization of positions His-6 and Met-45, whereas Phe-50 was varied using NYK-codon degeneracy.[28–31] The NYK-codon degeneracy was chosen for position Phe-50 because it reduces the library size by covering only the codons of nine different aliphatic and polar amino acid residues, including those residues which result in an enhanced aldolase activity (Ala, Val and Ile), as well as the wild-type residue (Phe). In addition to this triple-site library, a double-site library was constructed by varying positions Met-45 and Phe-50 simultaneously using NNK-codon degeneracy for both positions. Positions Met-45 and Phe-50 were chosen for this double-site library as single mutations at these positions resulted in higher aldolase activity as compared to the activity of single mutants at position His-6 (Figure 4.2).

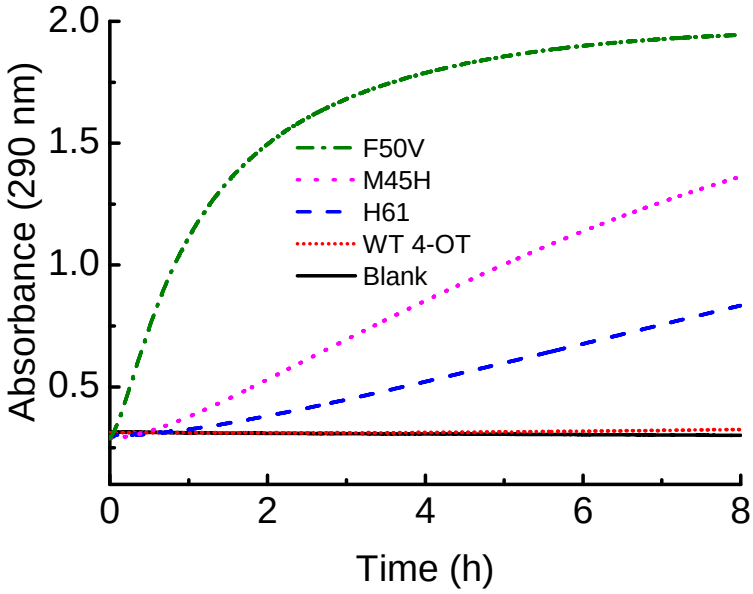

Figure 4.2: UV traces monitoring the formation of cinnamaldehyde (**6**) from acetaldehyde (**3**) and benzaldehyde (**4**) in the absence of enzyme (blank) or in the presence of purified wild-type 4-OT, 4-OT H6I, 4-OT M45H or 4-OT F50V.

The two libraries were used to transform Escherichia coli cells. The double-site library was screened by evaluating ∼3500 transformants, whereas ∼3500 transformants of the triple-site library were screened for the aldol condensation of **3** and **4**. Activity screening of the two libraries resulted in the identification of two mutants (M45T/F50A from the double-site library and H6F/M45T/F50A from the triple-site library) that showed a significant improvement in aldolase activity compared to that of the best single mutant F50V (which was used as a control in the screening assays). The progress curves of the aldol condensation of **3** (50 mM) with **4** (2 mM) catalyzed by the purified enzymes confirmed the enhanced activities of mutants M45T/F50A and H6F/M45T/F50A when compared to wild-type 4-OT and mutant F50V (Figure 4.3). ^{1}H NMR spectroscopic analysis confirmed that product **6** is formed in the aldol condensation of **3** with **4** catalyzed by mutant F50V, M45T/F50A or H6F/M45T/F50A (Figure 4.S3).

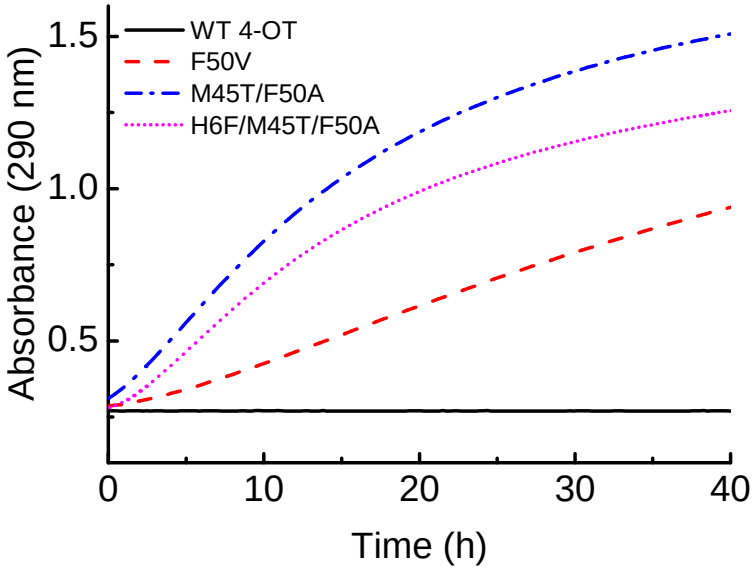

Figure 4.3: UV traces monitoring the formation of cinnamaldehyde (**6**) from acetaldehyde (**3**) and benzaldehyde (**4**) in the presence of purified wild-type 4-OT, 4-OT F50V, 4-OT M45T/F50A or 4-OT H6F/M45T/F50A.

Having established that mutants F50V, M45T/F50A and H6F/M45T/F50A have greatly improved aldolase activity, apparent kinetic parameters were determined using a fixed concentration of **3** (50 mM) and varying concentrations of **4** (0.1 - 15 mM). As shown in Table 4.1, the catalytic efficiency (in terms of k_{cat}/K_m) of the single mutant F50V is 640-fold higher than that of the wild-type 4-OT. Strikingly, the catalytic efficiencies of the double mutant M45T/F50A and the triple mutant H6F/M45T/F50A are 3300-fold and ∼5300-fold higher than that of wild-type 4-OT, respectively. The improved catalytic

Table 4.1: Apparent kinetic parameters for the aldol condensation of **3** and **4**, to yield **6**, catalyzed by wild-type 4-OT and 4-OT variants

Enzyme	k_{cat} (min^{-1})	K_m for **4** (mM)	k_{cat}/K_m (M^{-1} min^{-1})	Relative (k_{cat}/K_m)
Wild-type	n.d.[a]	n.d. [a]	5.08×10^{-2}	1
F50V	0.27 ± 0.01	8.4 ± 0.8	32	636
M45T/F50A	0.28 ± 0.008	1.7 ± 0.1	168	3300
H6F/M45T/F50A	0.19 ± 0.005	0.7 ± 0.06	268	5276

[a]n.d., not determined.

efficiencies of the double and triple mutants, when compared to the single mutant F50V, are due to a lowered K_m value for substrate **4**.

Next, we chemically synthesized compound **5**[12,32] and assessed the ability of mutants F50V, M45T/F50A and H6F/M45T/F50A to catalyze dehydration and retro-aldol reactions with this substrate. UV spectroscopic analysis revealed increases in absorbance at 250 nm and 290 nm (Figure 4.S4). The increase in absorbance at 290 nm corresponds to the formation of **6**, which results from the dehydration of **5**. The increase in absorbance at 250 nm corresponds to the formation of **4**, which results from the retro-aldol cleavage of **5**. Interestingly, while mutants M45T/F50A and H6F/M45T/F50A catalyze both retro-aldol and dehydration reactions using **5** as the substrate, mutant F50V appears to mainly catalyze the dehydration reaction (Figure 4.S4). All three mutants showed a strongly improved activity with substrate **5** as compared to wild-type 4-OT. Notably, additional increases in absorbance at 227 nm, which corresponds to the formation of but-2-enal (*i.e.*, the product of the self-condensation of **3**),[10] were observed in samples containing the mutant enzymes, indicating the formation of **3** during the course of the retro-aldol reactions.

^{1}H NMR spectroscopic analysis confirmed the enhanced activity of the three mutant enzymes for substrate **5** when compared to wild-type 4-OT (Figure 4.S5). After 18 h of incubation, compound **5** was fully converted by the three mutant enzymes, while only 34% conversion (26% conversion of **5** into **6** and 8% conversion of **5** into **3** and **4**) was observed in the reaction mixture with wild-type 4-OT. The ^{1}H NMR data confirmed that mutant F50V mainly catalyzes the dehydration reaction (65% dehydration versus 35% retro-aldol reaction), and demonstrated that mutants M45T/F50A (28% dehydration versus 72% retro-aldol reaction) and H6F/M45T/F50A (21% dehydration versus 79% retro-aldol reaction) mainly catalyze the retroaldol cleavage of **5**. These results

Table 4.2: Kinetic parameters for the ketonization of **1**, to yield **2**, catalyzed by wild-type 4-OT and 4-OT variants

Enzyme	k_{cat} (s^{-1})	K_m (μM)	k_{cat}/K_m (M^{-1} s^{-1})	Relative (k_{cat}/K_m)
Wild-type	1433 ± 35	31 ± 2	4.6×10^7	1
F50V	134 ± 1	253 ± 6	5.3×10^5	$(87)^{-1}$
M45T/F50A	n.d.[a]	n.d.[a]	8.0×10^3	$(5750)^{-1}$
H6F/M45T/F50A	n.d.[a]	n.d.[a]	9.4×10^3	$(4893)^{-1}$

[a]n.d., not determined.

surprisingly demonstrate that the double and triple mutants have an inverted reaction specificity as compared to wild-type 4-OT and the single mutant F50V.

Finally, we examined whether the engineered 4-OT variants (F50V, M45T/F50A, and H6F/M45T/F50A) still possess native tautomerase activity. Accordingly, kinetic parameters were determined using varying concentrations of the natural substrate **1** (Table 4.2).[5] With 87-, 5750- and 4893-fold decreases in k_{cat}/K_m for the F50V-, M45T/F50A- and H6F/M45T/F50A-catalyzed tautomerization reactions, respectively, these mutants have a largely decreased catalytic efficiency compared to that of the wild-type 4-OT. Notably, the mutations M45T/F50A and H6F/M45T/F50A resulted in enzymes with a$>10^7$-fold change in reaction specificity. Hence, the large increase in promiscuous aldolase activity for these mutants is accompanied by a large decrease in natural tautomerase activity, indicating a strong negative tradeoff between evolving and existing activity.[33–37]

4.3 Conclusion

In summary, we demonstrated that the promiscuous enzyme 4-OT can be engineered into a more efficient aldolase by exploring small libraries in which only 'hotspot' positions are varied. The 'hotspot' positions were identified by a systematic mutagenesis strategy, covering each residue position, followed by a screen for single mutations that give a marked improvement in the desired aldolase activity. These mutations were all found to be near the active site, providing direct support for the notion that for new

catalytic activities in a promiscuous enzyme, mutations closer to the active site improve the enzyme more effectively than distant ones.[23] In future work, we aim to explore the substrate scope of the engineered 4-OT variants, focusing on challenging aldol reactions between two aldehydes, and design new 4-OT variants that lack dehydration activity but possess further enhanced aldolase activity. To support the latter goal and to place our engineering efforts into a structural context, work is in progress to determine the crystal structures of 4-OT and the best 4-OT variants in complex with the unnatural substrate **5** or product **6**.

References

[1] G. J. Poelarends, V. Puthan Veetil, C. P. Whitman, *Cell. Mol. Life Sci.* 2008, 65, 3606-3618.

[2] B.-J. Baas, E. Zandvoort, E. M. Geertsema, G. J. Poelarends, *Chembiochem* 2013, 14, 917-926.

[3] C. P. Whitman, *Arch. Biochem. Biophys.* 2002, 402, 1-13.

[4] S. Harayama, M. Rekik, K. L. Ngai, L. N. Ornston, *J. Bacteriol.* 1989, 171, 6251-6258.

[5] C. P. Whitman, B. A. Aird, W. R. Gillespie, N. J. Stolowich, *J. Am. Chem. Soc.* 1991, 113, 3154-3162.

[6] J. T. Stivers, C. Abeygunawardana, A. S. Mildvan, G. Hajipour, C. P. Whitman, *Biochemistry* 1996, 35, 814-823.

[7] Y. Miao, M. Rahimi, E. M. Geertsema, G. J. Poelarends, *Curr. Opin. Chem. Biol.* 2015, 25, 115-23.

[8] E. Zandvoort, E. M. Geertsema, B.-J. Baas, W. J. Quax, G. J. Poelarends, *Chembiochem* 2012, 13, 1869-1873.

[9] Y. Miao, E. M. Geertsema, P. G. Tepper, E. Zandvoort, G. J. Poelarends, *Chembiochem* 2013, 14, 191-194.

[10] E. Zandvoort, B.-J. Baas, W. J. Quax, G. J. Poelarends, *Chembiochem* 2011, 12, 602-609.

[11] E. Zandvoort, E. M. Geertsema, B.-J. Baas, W. J. Quax, G. J. Poelarends, *Angew. Chem. Int. Ed. Engl.* 2012, 51, 1240-1243.

[12] E. Zandvoort, E. M. Geertsema, W. J. Quax, G. J. Poelarends, *Chembiochem* 2012, 13, 1274-1277.

[13] E. M. Geertsema, Y. Miao, P. G. Tepper, P. de Haan, E. Zandvoort, G. J. Poelarends, *Chem. Eur. J.* 2013, 19, 14407-14410.

[14] E. M. Geertsema, Y. Miao, G. J. Poelarends, *Practical Methods in Biocatalysis and Biotransformations*, Vol. 3 (Eds: J. Whittal, P. Sutton, W. Kroutil), Wiley, UK., 2014.

[15] E. M. Geertsema, G. J. Poelarends, *in Science of Synthesis: Biocatalysis in Organic Synthesis,* Vol. 2 (Eds: K. Faber, W. D. Fessner, N. Turner), Thieme Chemistry, Stuttgart, Germany, p.313-333, 2014.

[16] M. Rahimi, E. M. Geertsema, Y. Miao, J.-Y. van der Meer, T. van der Bosch, P. de Haan, E. Zandvoort, G. J. Poelarends, 2015, *unpublished data*.

[17] H. Poddar, M. Rahimi, E. M. Geertsema, A.-M. W. H. Thunnissen, G. J. Poelarends, *ChemBioChem* 2015, 16, 738-741.

[18] P. Y. Bruice, *Organic Chemistry*, 4th ed., Pearson Education, NJ, USA, 2004, Chapter 19.

[19] E. J. Corey, X. M. Cheng, *The Logic of Chemical Synthesis*, John Wiley & Sons, New York, 1989.

[20] V. Resch, J. H. Schrittwieser, E. Siirola, W. Kroutil, *Curr. Opin. Biotechnol.* 2011, 22, 793-799.

[21] T. D. Machajewski, C.-H. Wong, *Angew. Chem. Int. Ed. Engl.* 2000, 39, 1352-1375.

[22] P. Clapés, W.-D. Fessner, G. A Sprenger, A. K. Samland, *Curr. Opin. Chem. Biol.* 2010, 14, 154-167.

[23] K. L Morley, R.J. Kazlauskas, T*rends Biotechnol.* 2005, 23, 231-237.

[24] S.G. Peisajovich, D.S. Tawfik, *Nature Methods* 2007, 4, 991-994.

[25] Y. Yoshikuni, T. E. Ferrin, J. D. Keasling, *Nature* 2006, 440, 1078-1082.

[26] D. M. Z. Schmidt, E. C. Mundorff, M. Dojka, E. Bermudez, J. E. Ness, S. Govindarajan, P. C. Babbitt, J. Minshull, *J. A. Gerlt, Biochemistry* 2003, 42, 8387-8393.

[27] J.-Y. van der Meer, H. Poddar, B.-J. Baas, Y. Miao, M. Rahimi, A. Kunzendorf, R. van Merkerk, P. G. Tepper, E. M. Geertsema, A.-M.W.H. Tunnissen, W. J. Quax, G. J. Poelarends, 2015, *manuscript submitted.*

[28] M. T. Reetz, M. Bocola, J. D. Carballeira, D. Zha, A. Vogel, *Angew. Chem. Int. Ed. Engl.* 2005, 44, 4192-4196.

[29] M. T. Reetz, J. D. Carballeira, J. Peyralans, H. HG'Abenreich, A. Maichele, A. Vogel, *Chem. Eur. J.* 2006, 12, 6031-6038.

[30] M. T. Reetz, L. W. Wang, M. Bocola, *Angew. Chem. Int. Ed. Engl.* 2006, 45, 1236-1241.

[31] M. T. Reetz, D. Kahakeaw, R. Lohmer, *ChemBioChem* 2008, 9, 1797-1804.

[32] S. Couty, C. Meyer, J. Cossy, *Tetrahedron* 2009, 65, 1809-1832.

[33] M. Soskine, D. S. Tawfik, *Nat. Rev. Genet.* 2010, 11, 572-582.

[34] O. Khersonsky, D. S. Tawfik, *Annu. Rev. Biochem.* 2010, 79, 471-505.

[35] O. Khersonsky, C. Roodveldt, D. S. Tawfik, *Curr. Opin. Chem. Biol.* 2006, 10, 498-508.

[36] A. Aharoni, L. Gaidukov, O. Khersonsky, S. McQ Gould, C. Roodveldt, D. S. Tawfik, *Nat. Genet.* 2005, 37, 73-76.

[37] N. Tokuriki, C. J. Jackson, L. Afriat-Jurnou, K. T. Wyganowski, R. Tang, D. S. Tawfik, *Nat. Commun.* 2012, 3, 1257.

4.A Supplementary Information

Materials:

The sources for the buffers, solvents, components of Luria-Bertani (LB) media, as well as the materials, enzymes and reagents exploited in molecular biology procedures are reported elsewhere.[1]

General methods:

Standard molecular biology techniques were performed based on methods described elsewhere.[2] Protein was analyzed by polyacrylamide gel electrophoresis (PAGE) using pre-casted 10% polyacrylamide gels (NuPAGE®) Novex®) 10% Bis-Tris). Coomassie brilliant blue was used to stain the gels. Protein concentrations were determined using the Waddell method.[3] Enzymatic assays were performed either on a V-650 or V-660 spectrophotometer from Jasco (IJsselstein, The Netherlands) or on a SPECTROstar Omega plate reader (BMG LABTECH, Isogen Life Science, de Meern, NL). ^{1}H NMR spectra were recorded on a Varian Inova 500 (500 MHz) spectrometer using a pulse sequence for selective presaturation of the water signal. Chemical shifts for protons are reported in parts per million scale and are referenced to H_2O (δ= 4.80).

Expression and purification of 4-OT wild-type and mutants:

All 4-OT enzymes were produced in *E. coli* BL21(DE3), as native proteins without any affinity tag, using the pET20b(+) expression system as described before.[4] The construction of the expression vector for the production of 4-OT and the purification procedure for this enzyme have been reported previously.[4] To confirm that the proteins had been processed correctly and the initiating methionine had been removed, the masses of purified 4-OT wild-type and mutants were determined by ESI-MS.

Preparation of 1040 single 4-OT mutants:

Preparation of 1040 single 4-OT mutants: A defined collection of 1040 single mutant 4-OT genes, each cloned individually into a pJexpress 414 vector, was purchased from DNA2.0 (Menlo Park, CA).[5] This collection covered at least 15 of the 19 possible variants on each residue position, ranging from Ile-2 to the carboxy-terminal Arg-62. Single mutants of the amino-terminal proline residue (Pro-1) were not included in the collection, because Pro-1 is a key catalytic residue and mutations at this position lead to incorrect demethionylation of the protein.[5] In total 90% of all possible single 4-OT mutants is present in this collection. An aliquot of each pJexpress 414 vector with a unique mutant 4-OT gene was transformed individually into *E. coli* BL21(DE3), as described elsewhere.[5] Each *E. coli* BL21(DE3) transformant harboring a pJexpress 414 vector with a unique mutant 4-OT gene was stored at -80° until further use.

Cell-free extract preparation and 4-OT concentration assessment:

The expression levels and activities of all members of the 4-OT mutant collection were determined using cell-free extracts (CFEs) of cultures each expressing a different 4-OT mutant. Aliquots of the -80°C stock of the transformed *E. coli* BL21(DE3) cells were placed into wells of 96-deep-well plates (Greiner Bio-one, 96 well Masterblock®). Each mutant was placed into two wells as a duplicate. Each well contained 1.25 mL LB, supplemented with 100 µg/mL ampicillin and 100 µM isopropyl-β-D-1-thiogalactopyranoside (IPTG) as inducer. The deep-well plates with inoculated LB medium were sealed with sterile, gas-permeable seals (Greiner Bio-one, BREATHseal™) and incubated overnight at 37°C with shaking at 250 rpm. After the incubation, the cultures were pelleted at 3500 RPM for 30 min at 4°C. The pellets of the duplicates were pooled and lysed with 375 µl BugBuster™ (Novagen), which was supplemented with 25 U/mL benzonase nuclease. The cells were lysed at room temperature for 20 minutes with vigorous shaking. The cell lysates were cleared by centrifugation at 4000 RPM for 20 minutes at 4°C, after which the CFE was obtained as the supernatant. The 4-OT concentration in each CFE was determined using a quantitative densitometric analysis as described before.[5]

Determination of the aldolase activity of the single 4-OT mutants:

The produced CFEs were used to determine the aldolase activity of the single mutants of 4-OT using UV-spectroscopy. The UV-spectroscopic measurements were performed in 96-wells micro titer plates (MTPs) (UV-star µclear, Greiner Bio-one). The reaction mixtures consisted of CFE (30% v/v), acetaldehyde (**3**, 50 mM) and benzaldehyde (**4**, 2 mM) in 10 mM NaH_2PO_4 buffer (pH 7.3). The volume of these reaction mixtures was 100 µL and the MTPs were sealed with UV-transparent plate seals (VIEWsealTM, Greiner Bio-one) to eliminate evaporation. The MPTs were incubated for 16 h at 25°C during which the reaction progress was monitored by UV-spectroscopy (220-500 nm). Formation of product **6** (λ_{max} = 290 nm) was quantified based on the increase in absorbance at 290 nm after 16 h. To eliminate false positives in which the increase in absorbance at 290 nm was a result of protein precipitation (in these cases there is an increase in absorbance over the whole range of the UV-spectrum), the ΔA290 values are corrected for absorbance changes at 350 nm. At this wavelength product **6** has no UV-absorbance. Reaction mixtures in which there was a high increase of absorbance at 350 nm ($\Delta A_{350} > 0.5$) were assigned as "precipitation" (Figure 4.1). The low-level aldolase activity of wild-type 4-OT was below the detection limit of this assay. Therefore, only single mutants with a strongly improved aldolase activity were identified. Using Microsoft excel 2010, the activity data were represented as colors in the data matrix to create a visually interpretable heat map (Figure 4.1).

Construction of double- and triple-site mutant libraries:

4-OT mutant libraries were constructed by PCR, using the coding sequence for 4-OT in plasmid pET20b (4-OT) as the template. For the Met45NNK/Phe50NNK library the following primers were used: F5′-A TAG CAG GTA CAT ATG CCT ATT GCC CAG ATC CAC ATC-3′ and R5′-A TGT TAT GGA TCC TCA GCG TCT GAC CTT GCT GGC CAG TTC GCC GCC GAT GCC **MNN** GTG GCC CTT GGC **MNN** CTC CGT-3′. For the H6NNK/Met45NNK/Phe50NYK library the following primers were used: F5′-A TAG CAG GTA CAT ATG CCT ATT GCC CAG ATC **NNK** ATC CTT GAA GGC-3′ and R5′-A TGT TAT GGA TCC TCA GCG TCT GAC CTT GCT GGC CAG TTC GCC GCC GAT GCC **MRN** GTG GCC CTT GGC **MNN** CTC CGT-3′. Mutated codons are in bold and restriction sites are underlined. The following PCR program was used: 95°C (denaturation, 2 min), 55°C (annealing, 1 min), 72°C (elongation, 1 min) for 35 cycles, followed by a final elongation step (72°C, 10 min). The resulting PCR products were gel purified, digested, and cloned in frame with the ATG start codon of the pET20b(+) vector. The ligation mixtures were used to transform competent *E. coli* DH10B cells using electroporation. The transformants were selected overnight at 37°C on LB-agar plates supplemented with 100 µg/mL ampicillin. Plasmid DNA was extracted from randomly picked colonies and the 4-OT gene was fully sequenced to assure that the desired mutations were introduced. After having established that the libraries were of good quality, all colonies were collected into 10 mL LB and cells were harvested by centrifugation (13000g, 10 min). From these cells, plasmid DNA was isolated and subsequently transformed into *E. coli* BL21(DE3) cells to express the mutant 4-OT genes.

Activity screening of double- and triple-site mutant libraries:

Colonies of *E. coli* BL21(DE3) expressing the mutant 4-OT genes were picked individually and grown overnight at 37°C in 96-deep-well plates containing 1.25 mL LB medium supplemented with 100 µg/mL ampicillin. Colonies expressing F50V (positive control) or wild-type 4-OT and colonies containing empty plasmids (negative control) were also picked and grown overnight in each 96-deep well plate. The cells were collected by centrifugation (3500 rpm, 30 min, 4°C) and lysed with BugBuster^{TM} (200 µL per well, 20 min incubation with vigorous shaking) containing benzonase nuclease (25 U/mL). The cell lysate was cleared by centrifugation (4000 rpm, 30 min, 4°C), after which the CFE was obtained as the supernatant. An aliquot of each CFE (30 µL) was transferred into a well of a MTP and incubated with 50 mM **3** and 2 mM **4** in 20 mM NaH_2PO_4 buffer (pH 7.3). The final volume of each reaction mixture was 100 X′Ol. The MTPs were sealed with UV-transparent plate seals and reaction progress was monitored by UV-spectroscopy as decribed above.

UV-spectroscopic assay for the aldolase activity of purified enzymes:

The aldolase activity of purified wild-type 4-OT and 4-OT mutants was monitored by following the increase in absorbance at 290 nm, which corresponds to the formation of cinnamaldehyde (**6**) (ε = 26.7 mM^{-1} cm^{-1}). Purified enzyme (300 µg, 149 µM) was incubated in a 1 mm cuvette with **3** (50 mM) and **4** (2 mM) in 20 mM NaH_2PO_4 buffer (pH 7.3; 0.3 mL final volume). Absorbance spectra were recorded from 200 to 400 nm (Figure 4.S2).

Procedure for progress curve analysis:

The reaction progress of the aldol condensation of **3** with **4** catalyzed by purified wild-type 4-OT or 4-OT mutants was monitored by following the increase in absorbance at 290 nm, which corresponds to the formation of **6**. An aliquot of purified enzyme was added to NaH_2PO_4 buffer (0.3 mL, 20 mM; pH 7.3) in a 1 mm cuvette, yielding a final enzyme concentration of 1 mg/mL. The final concentrations of **3** and **4** were 50 and 2 mM, respectively. To obtain the progress curves, the increase in absorbance was plotted against time (Figures 4.2 and 4.3).

^{1}H NMR spectroscopic assay for aldolase activity:

In separate experiments, wild-type 4-OT and the 4-OT mutants F50V, M45T/F50A and H6F/M45T/F50A (1 mg/mL, 150 µM in 20 mM NaH_2PO_4, pH 7.3) were incubated with **3** (30 mM in 20 mM NaD_2PO_4, pD 7.5), **4** (15 mM in 20 mM NaD_2PO_4, pD 7.5) and 18-crown-6 (internal standard; 3.75 mM), and the reaction progress was monitored by ^{1}H NMR spectroscopy. In addition, a control sample was prepared with all the components except for the enzyme. The first ^{1}H NMR spectrum was recorded immediately after mixing, and then after 1 and 4 d (Figure 4.S3). The ^{1}H NMR signals for **3** (and its hydrate), **4**, **6** and internal standard are reported below.

Compound 3 and its hydrate (3'):1H NMR (500 MHz, 20 mM NaD2PO4; pD 7.6): δ9.69 (t, *J* = 1.3 Hz, 1H), 2.57 (dq, *J* = 7.3, 1.3 Hz, 2H), 1.06 (t, *J* = 7.3 Hz, 3H).

Compound 4: ^{1}H NMR (500 MHz, D_2O, 25°C): δ= 9.94 (s, 1H), 7.96 (d, *J* = 8.0 Hz, 2H), 7.76 (t, *J* = 7.5 Hz, 1H), 7.63 (t, *J* = 7.5 Hz, 2H).

Compound 6: ^{1}H NMR (500 MHz, D_2O, 25°C): δ= 9.57 (d, *J* = 8.0 Hz, 1H), 7.80 (d, *J* = 15.5 Hz, 1H), 7.74 (d, *J* = 8.0 Hz, 2H), 7.52 (m, 3H), 6.84 (dd, *J* = 8.0, 8.0 Hz, 1H).

Internal standard 18-crown-6 (1,4,7,10,13,16-hexaoxacyclooctadecane): ^{1}H NMR (500 MHz, 20 mM NaD_2PO_4; pD 7.6): δ= 3.68 (s, 24H)

Chemical synthesis of compound 5:

The chemical synthesis of 3-hydroxy-3-phenylpropanal (**5**) has been described elsewhere.[6]

UV-spectroscopic assay for monitoring dehydration and retro-aldol cleavage of 5:

The retro-aldol and dehydration activities of wild-type 4-OT and 4-OT mutants were monitored by following the formation of **6** and **4** by UV-spectroscopy. In separate experiments, wild-type 4-OT and 4-OT mutants F50V, M45T/F50A and H6F/M45T/F50A (1 mg/mL, 150 µM) were incubated with **5** (2 mM) in 20 mM NaH_2PO_4 buffer (pH 7.3; 0.3 mL final volume in a 1 mm cuvette). Absorbance spectra of the reaction mixtures were recorded from 200-400 nm every three minutes (Figure 4.S4).

^{1}H NMR spectroscopic assay for monitoring dehydration and retro-aldol cleavage of 5:

^{1}H NMR spectra monitoring the conversion of **5** into **3** and **4** (retro-aldolase activity) and **6** (dehydration activity) catalyzed by wild-type 4-OT and 4-OT mutants were recorded as follows. In separate experiments, wild-type 4-OT and 4-OT mutants F50V, M45T/F50A and H6F/M45T/F50A (1 mg/mL, 150 µM) were incubated with **5** (8.8 mM) and 18-crown-6 ether (internal standard, 1.1 mM) in 20 mM NaD_2PO_4, pD 7.5 (total volume of 650 µL). In addition, a control experiment without enzyme but with otherwise identical conditions was performed as well. The first ^{1}H NMR spectrum was recorded after 2 h, and then after 18 h (Figure 4.S5). The ^{1}H NMR signals observed for **3**, **4**, and **6** were in accordance with those of the corresponding standards. The ^{1}H NMR signals for **5** and its hydrated form are given below.

^{1}H NMR (300 MHz, D_2O, 25°C): 3-hydroxy-3-phenylpropanal (**5**); δ= 9.72 (dd, *J* = 1.9, 1.9 Hz, 1H), 7.49 - 7.34 (m, 5H), 5.32 (dd, *J* = 7.8, 5.4Hz, 1H), 3.04 (ddd, *J* = 17.1, 7.8, 1.9 Hz, 1H), 2.96 (ddd, *J* = 17.1, 5.4, 1.9 Hz, 1H)

3-phenylpropane-1,1,3-triol (**5'**, hydrated form of **5**); δ= 7.49 - 7.34 (m, 5H), 5.03 (dd, *J* = 6.0, 5.4 Hz, 1H), 4.85 (dd, *J* =8.4, 5.8 Hz, 1H), 2.15 (ddd, *J* = 13.9, 8.4, 5.4 Hz, 1H), 2.00 (ddd, *J* = 13.9, 6.0, 5.8 Hz, 1H).

Kinetics assays for aldolase activity:

The apparent kinetic parameters for the aldolase activity of wild-type 4-OT and 4-OT mutants were determined at 22°C by incubating the purified enzyme (150 µM) with a fixed concentration of **3** (50 mM) and varying concentrations of **4** (0.5 - 15 mM) in 20 mM NaH_2PO_4 buffer, pH 7.3 (final volume of 0.3 mL in a 1 mm cuvette). The reaction was monitored by following the increase in absorbance at 290 nm, which corresponds to the formation of **6**. The initial rates (mM/min) were plotted versus the concentration of **4** (mM). SigmaPlot was used to fit the data to Michaelis-Menten kinetics and to calculate the apparent kinetic parameters k_{cat} and K_m (for **4**).

Kinetic assays for tautomerase activity:

The tautomerase activity of wild-type 4-OT and 4-OT mutants was measured by monitoring the ketonization of 2-hydroxyhexa-2,4-dienedioate (**1**) to 2-oxohex-3-enedioate (**2**) in 20 mM NaH_2PO_4 buffer (pH 7.3) at 22 °C. Stock solutions of **1** were generated by dissolving the appropriate amount of **1** in absolute ethanol. The ketonization of **1** to **2** was monitored by following the increase in absorbance at 236 nm, which corresponds to the formation of **2** (ε = 6.58 $\times 10^3$ M^{-1} cm^{-1}). The assay was initiated by the addition of a small aliquot of **1** (2-15 µL) to 1 mL of the assay buffer containing an appropriate amount of enzyme. The initial rates (µM/s) were plotted versus the concentration of **1** (µM). SigmaPlot was used to fit the data to Michaelis-Menten kinetics and to calculate the kinetic parameters k_{cat} and K_m.

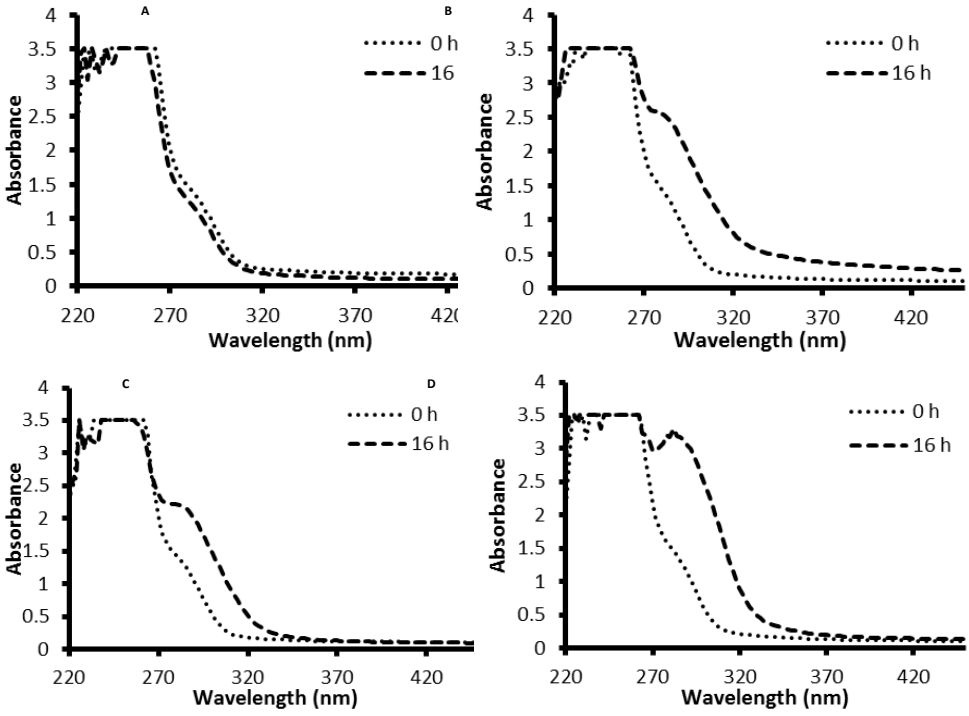

Figure 4.S1: UV spectra recorded after incubation of **3** and **4** (λ_{max} = 250 nm) with cell free extracts prepared from *E. coli* BL21(DE3) cultures expressing: A) wild type 4-OT; B) H6I; C) M45H and D) F50V. Formation of cinnamaldehyde (**6**) (λ_{max} = 290 nm) was monitored in the course of the reactions.

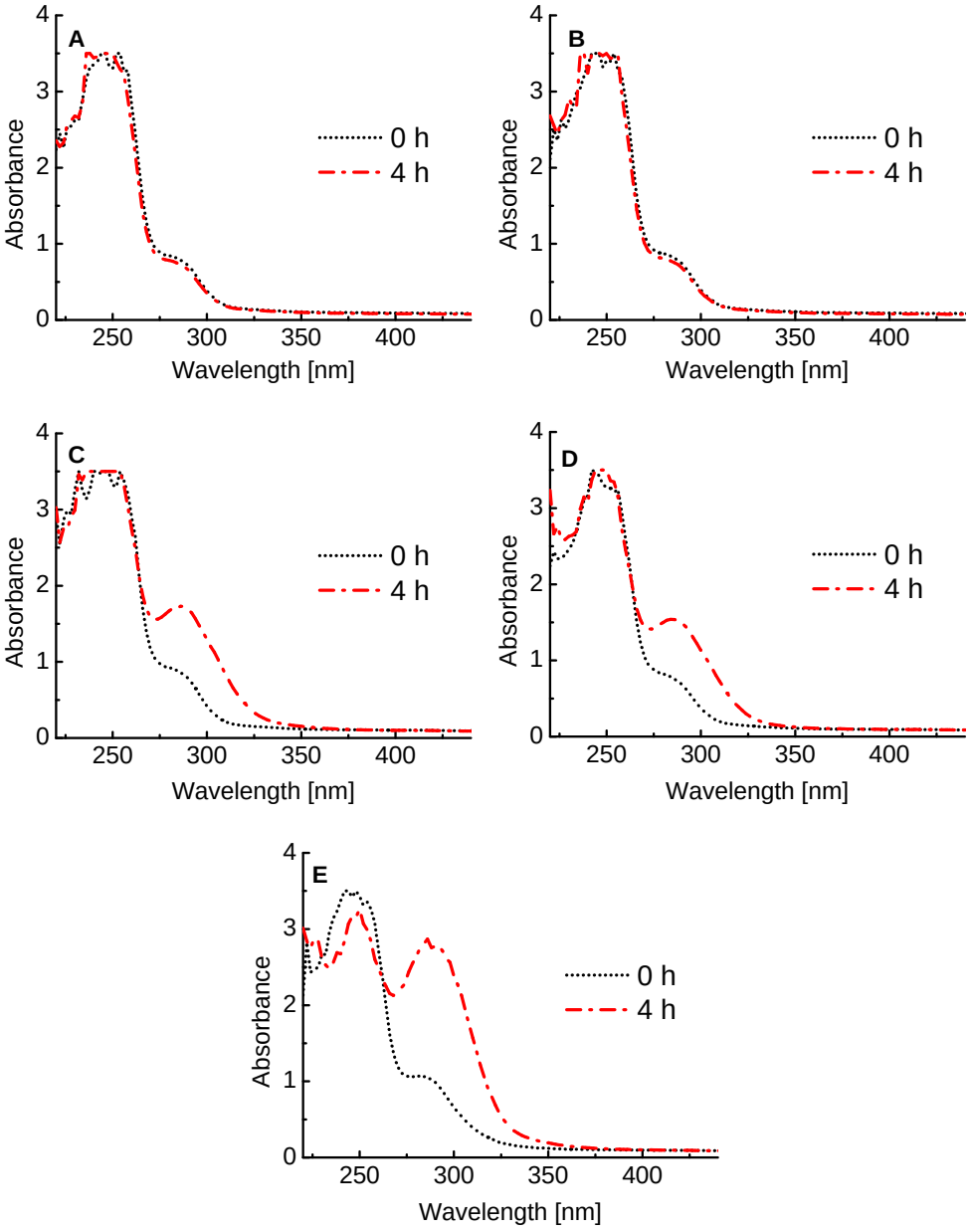

Figure 4.S2: UV spectra recorded after incubation of acetaldehyde (**3**) and benzaldehyde (**4**) (λ_{max} = 250 nm) with A) no enzyme (control sample); B) purified wild-type 4-OT; C) purified H6I; D) purified M45H; and E) purified F50V. Formation of cinnamaldehyde (**6**) (λ_{max} = 290 nm) was monitored in the course of the reactions.

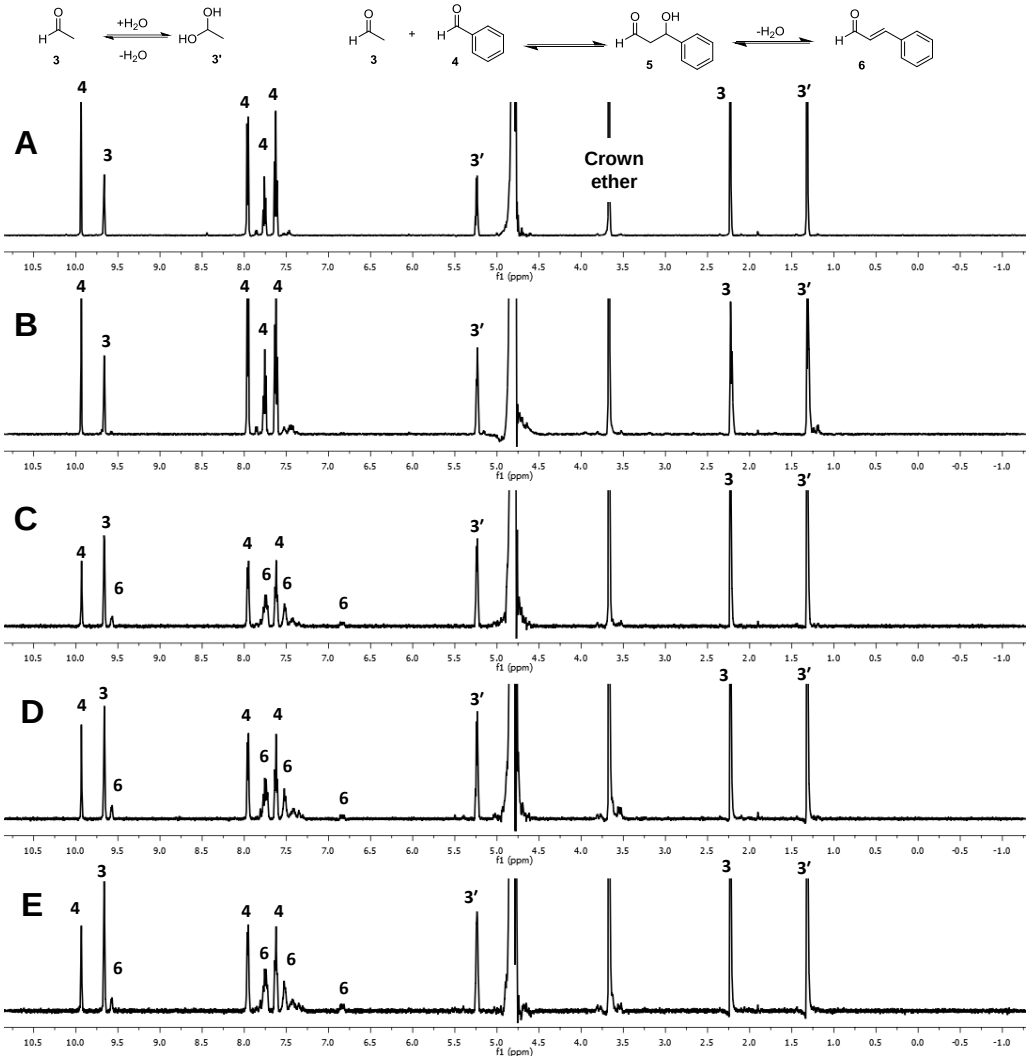

Figure 4.S3: Stack plot of ^{1}H NMR spectra recorded after 1 d of incubation of **3** and **4** with A) no enzyme; B) wild-type 4-OT; C) 4-OT F50V; D) 4-OT M45T/F50A; and E) 4-OT H6F/M45T/F50A. Signals corresponding to **3** and its hydrate (**3'**), **4** and **6** are marked.

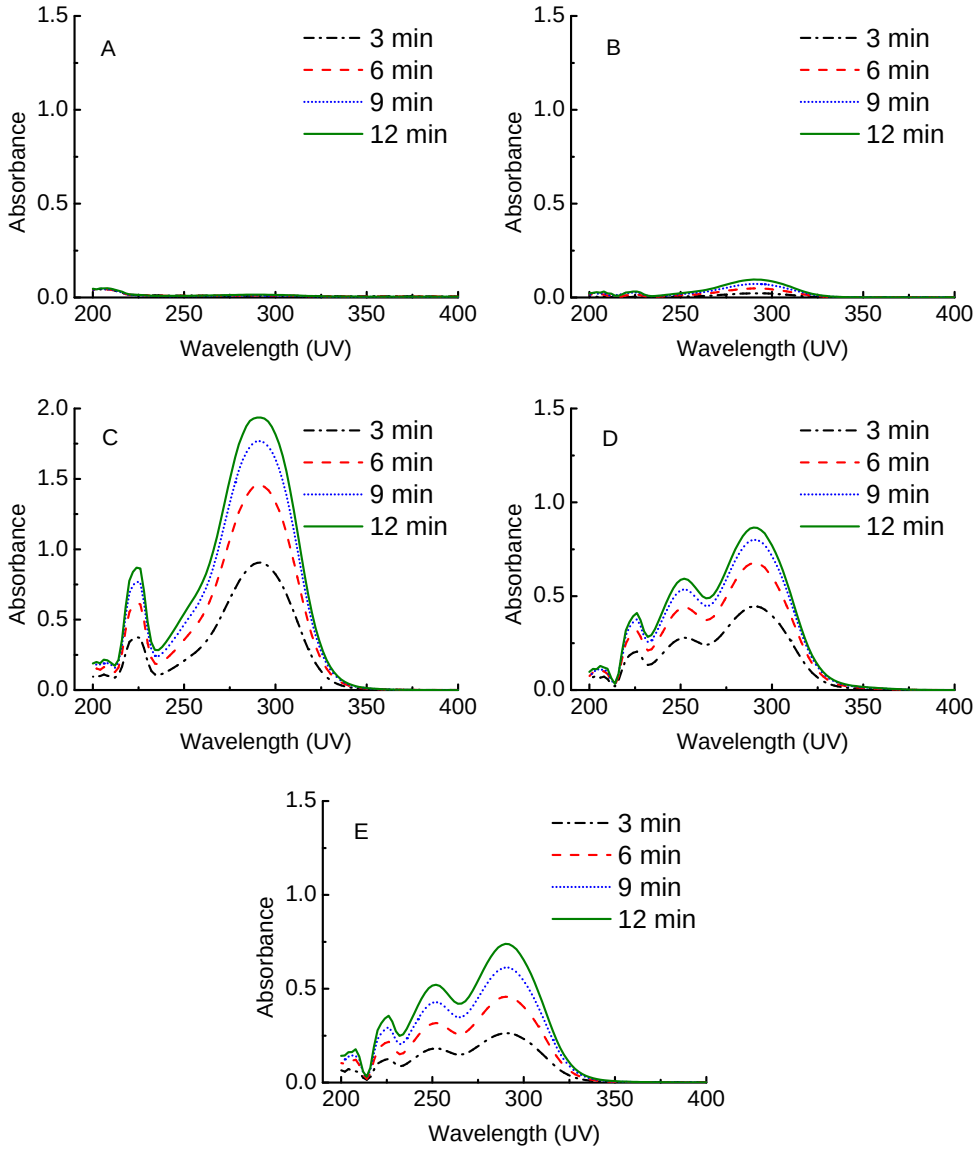

Figure 4.S4: UV spectra recorded after incubation of **5** (2 mM in 20 mM NaH_2PO_4 buffer at pH 7.3) with A) no enzyme (control sample); B) wild-type 4-OT; C) 4-OT F50V; D) 4-OT M45T/F50A; and E) 4-OT H6F/M45T/F50A.

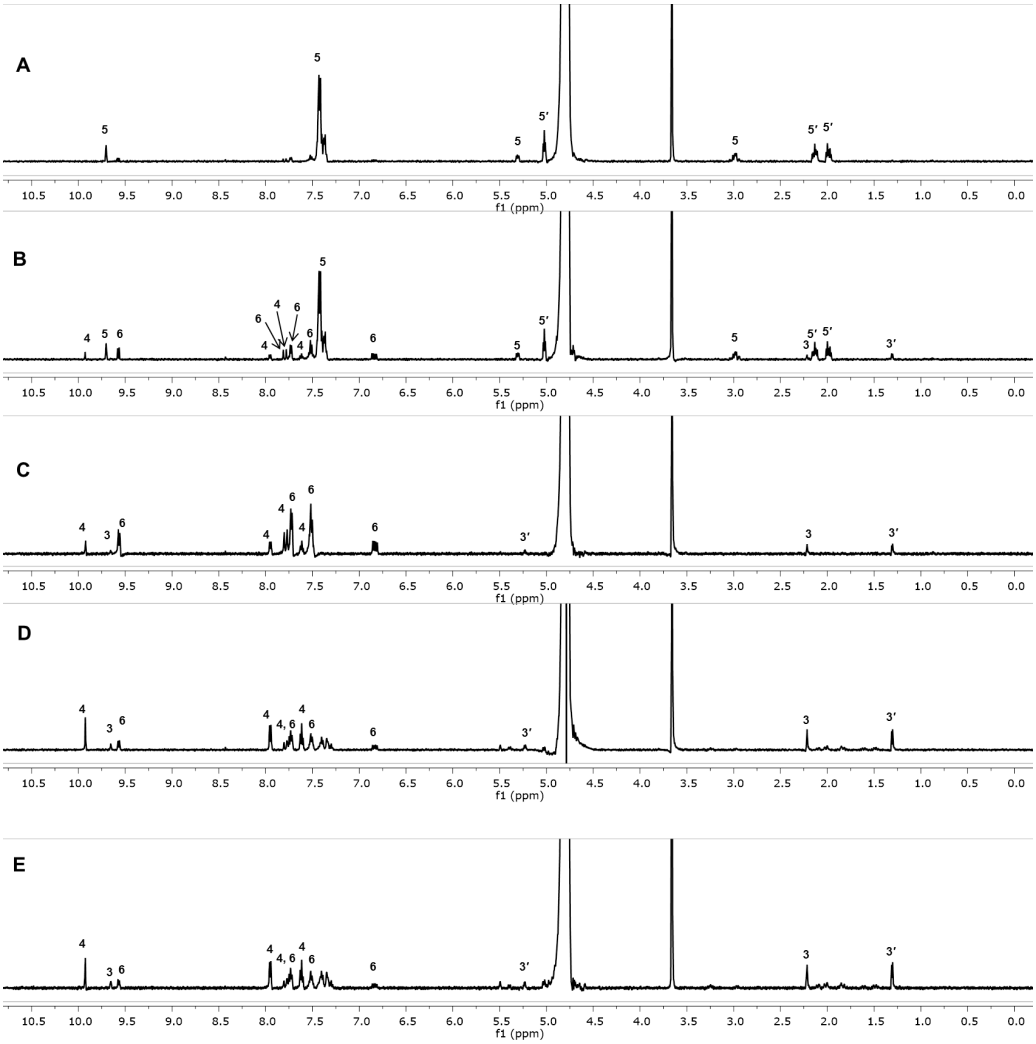

Figure 4.S5: Stack plot of ^{1}H NMR spectra recorded after 18 h of incubation of **5** with A) no enzyme; B) wild-type 4-OT; C) 4-OT F50V; D) 4-OT M45T/F50A; and E) 4-OT H6F/M45T/F50A. Signals corresponding to **3** and its hydrated (**3'**), **4**, **5** and its hydrate (**5'**), and **6** are marked.

References

[1] H. Raj, B. Weiner, V. Puthan Veetil, C. R. Reis, W. J. Quax, D. B. Janssen, B. L. Feringa, G. J. Poelarends, *ChemBioChem* 2009, 10, 2236-2245.

[2] J. Sambrook, E. F. Fritsch, T. Maniatis, *Molecular Cloning: A Laboratory Manual*. Cold Spring Harbor Laboratory Press, 1989.

[3] W. J. Waddell, *J. Lab. Clin. Med.* 1956, 48, 311-314.

[4] E. Zandvoort, B.-J. Baas, W. J. Quax, G. J. Poelarends, *Chembiochem* 2011, 12, 602-609.

[5] J.-Y. van der Meer, H. Poddar, B.-J. Baas, Y. Miao, M. Rahimi, A. Kunzendorf, R. van Merkerk, P. G. Tepper, E. M. Geertsema, A.-M.W.H. Thunnissen, W. J. Quax, G. J. Poelarends, *submitted for publication.*

[6] E. Zandvoort, E. M. Geertsema, W. J. Quax, G. J. Poelarends, *Chembiochem* 2012, 13, 1274-1277.